Available online at www.sciencedirect.com
ScienceDirect
Journal of Power Sources 167 (2007) 212–216
JOURNAL OF POWER SOURCES
www.elsevier.com/locate/jpowsour

Short communication

Electrochemical performance of $Li_{4/3}Ti_{5/3}O_4/Li_{1+x}(Ni_{1/3}Co_{1/3}Mn_{1/3})_{1-x}O_2$ cell for high power applications☆

W. Lu [a,1], J. Liu [a], Y.K. Sun [b], K. Amine [a,*]

[a] *Chemical Engineering Division, Argonne National Laboratory, 9700 S. Cass Avenue, Argonne, IL 60439, United States*
[b] *Division of Chemical Engineering, Hanyang University, 17 Haengdang-dong, Seongdong-gu, Seoul, Republic of Korea*

Received 25 September 2006; accepted 10 December 2006
Available online 16 January 2007

Abstract

A $Li_{4/3}Ti_{5/3}O_4/Li_{1+x}(Ni_{1/3}Co_{1/3}Mn_{1/3})_{1-x}O_2$ cell is shown to exhibit excellent cycling performance at both room and elevated temperature. This behaviour is attributed to the high stability of the $Li_{4/3}Ti_{5/3}O_4$ anode at the bulk structure level as well as at the interface, because there is no solid electrolyte interface effect. Moreover, it is found that the impedances of both materials are dominated by electrochemical kinetics (Butler–Volmer kinetics), which makes this a good system for high-power applications. The high voltage polarization of the $Li_{4/3}Ti_{5/3}O_4$ and $Li_{1+x}(Ni_{1/3}Co_{1/3}Mn_{1/3})_{1-x}O_2$ electrodes at the end of the charge and discharge gives a good indication of cell overcharge and overdischarge.

Keywords: Lithium-ion battery; Capacity retention; Cycle-life; $Li_{4/3}Ti_{5/3}O_4$; $Li_{1+x}(Ni_{1/3}Co_{1/3}Mn_{1/3})_{1-x}O_2$; High power

1. Introduction

$Li_{4/3}Ti_{5/3}O_4$ has been proposed as a promising negative-electrode (anode) candidate for lithium-ion batteries. This material is a member of the $Li_{1+x}Ti_{2-x}O_4$ ($0<x<1/3$) spinel family with two limiting compositions, namely, $LiTi_2O_4$ and $Li_{4/3}Ti_{5/3}O_4$. It is generally accepted that the $Li_{8a}[Li_{1/3}Ti_{5/3}]_{16d}O_4$ spinel will transform to the $[Li_2]_{16c}[Li_{1/3}Ti_{5/3}]_{16d}O_4$ rock–salt phase without a noticeable change in lattice dimension during the lithium insertion process [1]. Intensive studies have demonstrated [2–5] that cells based on this so-called zero-strain material exhibit excellent capacity retention during cycling [2–5]. Moreover, $Li_{4/3}Ti_{5/3}O_4$ has much better thermal stability compared with a carbonaceous anode due to its high operational redox potential [6,7].

$Li_{1+x}(Ni_{1/3}Co_{1/3}Mn_{1/3})_{1-x}O_2$ ($x=0.1$; denoted as L333) has been shown to be a promising positive-electrode (cathode) material for lithium-ion batteries, due to its long calendar life and cycle-life, excellent power capability, and good tolerance to thermal abuse [8–12].

This work reports the power capability and cycling performance at different temperatures of a cell based on L333 and $Li_{4/3}Ti_{5/3}O_4$ electrodes.

2. Experimental

The composition of the negative electrode is 80 wt.% $Li_{4/3}Ti_{5/3}O_4$ spinel (from Ishihara), 10 wt.% acetylene black, and 10 wt.% polyvinylidine difluoride (PVDF). The loading of the active material is 6.5 mg cm^{-2}, and the obtained capacity is about 1.89 mAh (175 mAh g^{-1}) for a (9/16)-in. electrode disc between 2.0 and 1.2 V versus Li/Li$^+$. The composition of the positive electrode is 82 wt.% L333, 10 wt.% TB5500, and 8 wt.% PVDF. The loading of active material is 7.2 mg cm^{-2}, and the obtained capacity is about 2.04 mAh (180 mAh g^{-1}) for a (9/16)-in. electrode disc between 3.2 and 4.3 V versus Li/Li$^+$.

☆ The submitted manuscript has been created by the University of Chicago as Operator of Argonne National Laboratory ("Argonne") under Contract No. W-31-109-ENG-38 with the U.S. Department of Energy. The U.S. Government retains for itself, and others acting on its behalf, a paid-up, nonexclusive, irrevocable worldwide license in said article to reproduce, prepare derivative works, distribute copies to the public, and perform publicly and display publicly, by or on behalf of the Government.

* Corresponding author. Tel.: +1 630 252 3838; +1 630 972 4451.
E-mail address: amine@cmt.anl.gov (K. Amine).
[1] Present address: 10,000 Wehrle Dr., Clarence, NY 14031.

0378-7753/$ – see front matter © 2007 Published by Elsevier B.V.
doi:10.1016/j.jpowsour.2006.12.077

A 2032-type coin cells (Li/$Li_{4/3}Ti_{5/3}O_4$, Li/L333, and $Li_{4/3}Ti_{5/3}O_4$/L333) were fabricated in a glove-box using a porous separator (Celgard 3501) and a 1.2 M $LiPF_6$ ethylene carbonate/ethyl methyl carbonate (EC/EMC) (3/7) electrolyte. The area of the electrode is 1.6 cm^2, and the cells were cycled by means of a Maccor system at different rates. The area-specific impedance (ASI) was measured during cycling with 30-s current interruptions. The $Li_{4/3}Ti_{5/3}O_4$/L333 cells were tested at both room and elevated (55 °C) temperatures. The ac impedance was measured at 50% state-of-charge (SoC) of the cell after different numbers of cycles.

3. Results and discussion

The voltage profiles of the Li/$Li_{4/3}Ti_{5/3}O_4$ and Li/L333 half-cells tested in this study are presented in Fig. 1(a). The irreversible capacity loss for the Li/L333 half-cell during the first formation cycle is about 12% (21 mAh g^{-1}). By contrast, the Li/$Li_{4/3}Ti_{5/3}O_4$ half-cell shows 100% columbic efficiency. There is a good correlation between the calculated and experimental voltage profiles of the $Li_{4/3}Ti_{5/3}O_4$/L333 cell, see Fig. 1(b). The calculated cell voltage profile in Fig. 1(a) was obtained by subtracting the half-cell voltage curve of the negative electrode from that of the positive electrode. The sharp increase in the cell potential at the end-of-charge (EoC) and the sharp decrease in the full-cell potential at the end-of-discharge (EoD) (Fig. 1(b)) can be attributed to the voltage drop of $Li_{4/3}Ti_{5/3}O_4$ and L333 at the EoC and EoD, respectively. This feature makes the cell, consisting of the $Li_{4/3}Ti_{5/3}O_4$ anode and L333 cathode, easier to balance and provides a better indication of the overcharge and overdischarge of the cell during cycling.

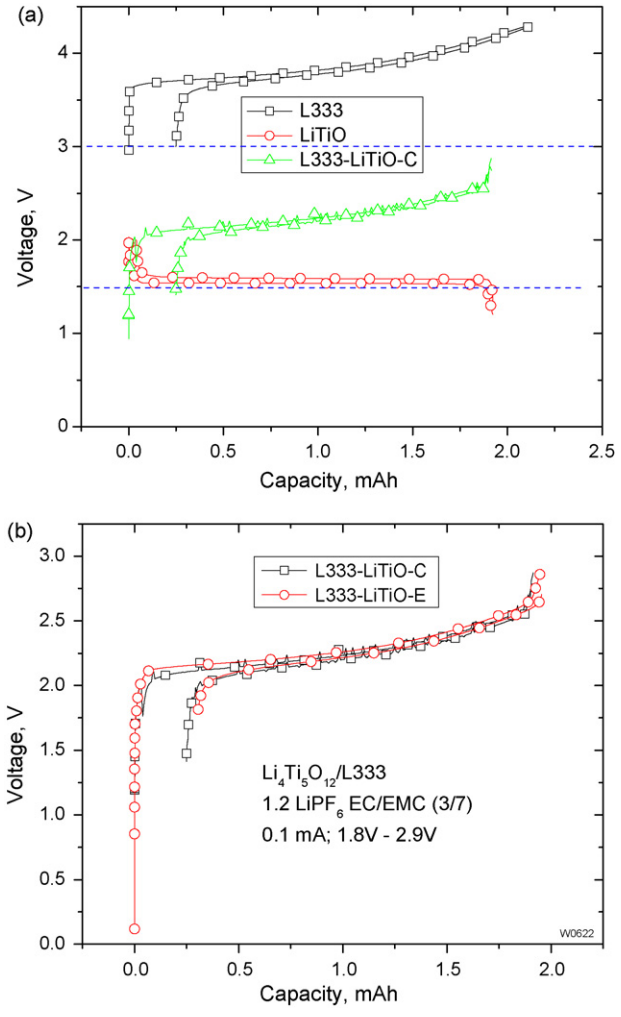

Fig. 1. Voltage profiles of (a) Li/L333 and Li/$Li_{4/3}Ti_{5/3}O_4$ cells and (b) $Li_{4/3}Ti_{5/3}O_4$/L333 cells from experiment and calculation.

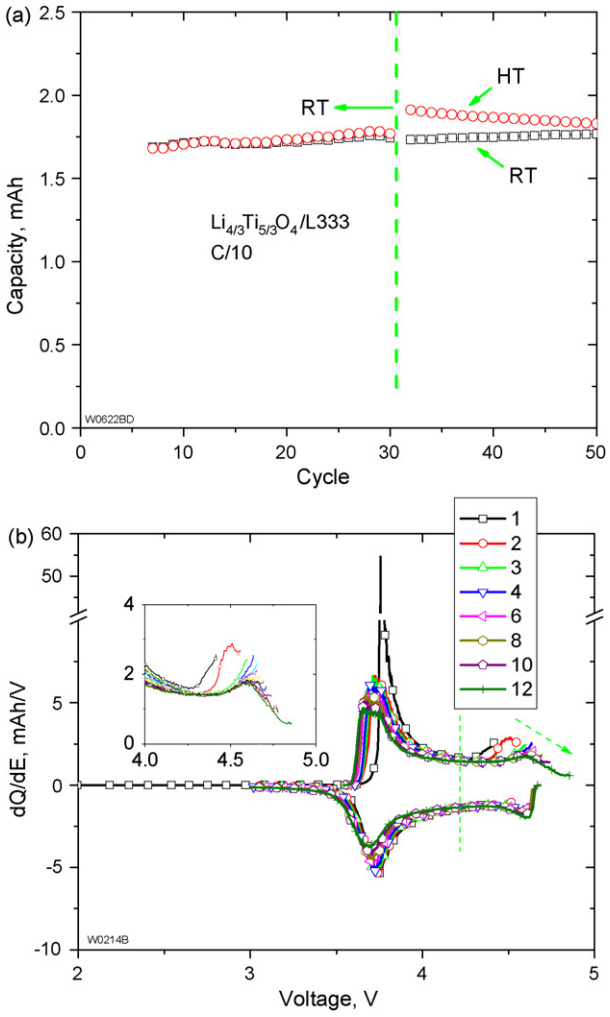

Fig. 2. (a) Capacity retention of $Li_{4/3}Ti_{5/3}O_4$/L333 cell at room temperature and elevated temperature at *C*/10 rate and (b) differential capacity plots of Li/L333 cell with 2.4 mAh capacity.

The cycling performance of the $Li_{4/3}Ti_{5/3}O_4$/L333 cell at room temperature and elevated temperature (55 °C) is shown in Fig. 2(a). Both cells were cycled at the *C*/10 rate at room temperature and exhibited the same capacity for 30 cycles. When the temperature of one of the two cells is increased to 55 °C, the capacity is increased slightly, and a continuous capacity fading is observed with cycling. This phenomenon can be explained by the differential capacity plot of the Li/L333 cell as a function of cell voltage shown in Fig. 2(b). In this test, the charging process is controlled by either the cell capacity

(2.4 mAh) or the voltage limit (4.9 V). During the first formation cycle, an irreversible peak starting at 4.3 V is observed. This irreversible peak shifts towards high potential during cycling and disappears once a new reversible redox reaction peak occurs above 4.6 V, where oxidation of Co^{3+} in the material takes place [13]. The irreversible peak has been reported previously with little discussion [14]. We believe that this irreversible capacity loss can be attributed to the removal of the excess lithium in the lithium-rich $Li_{1+x}(Ni_{1/3}Co_{1/3}Mn_{1/3})_{1-x}O_2$ material. The removed excess lithium cannot be inserted back into the structure and results in the irreversible capacity loss when the potential of L333 is above 4.3 V. Moreover, this irreversible extraction of excess lithium can take place at an earlier voltage when the cell is cycled at elevated temperature, due to better kinetics. The early extraction of additional lithium from the structure at 55 °C explains the higher capacity of the cell (Fig. 2(a)) when the temperature increases. Also, the irreversible extraction of lithium accounts for the capacity fading observed for the full-cell at 55 °C.

The 1*C* rate capacity retention of the $Li_{4/3}Ti_{5/3}O_4$/L333 cell at room and elevated temperatures is presented in Fig. 3(a). Under both test conditions, the capacity retention remains stable for over 200 cycles. The capacity retention of the $Li_{4/3}Ti_{5/3}O_4$/L333 system at 55 °C is about 96.5% after extensive cycling. This result is much better than that of the MCMB/L333 cell system, which shows only 83.5% capacity retention when subjected to the same test conditions. The high capacity retention of the $Li_{4/3}Ti_{5/3}O_4$/L333 cell can be attributed to the stability of the $Li_{4/3}Ti_{5/3}O_4$ negative electrode. The ac impedance spectra of the $Li_{4/3}Ti_{5/3}O_4$/L333 cell after the 70th and 220th cycle at 55 °C is shown in Fig. 3(b). Both spectra are identical, which indicates no interfacial reactivity is taking place during cycling at 55 °C. By contrast, cells with MCMB as the anode have been found [15,16] to show a significant rise in the interfacial impedance during cycling at 55 °C because of the instability of the solid electrolyte interface (SEI) film at such an elevated temperature. The cell performance study using a reference electrode also indicates that the capacity loss of the MCMB/L333 cell is due mainly to an increase in impedance of the anode during cycling [17].

The differential capacity plots of the $Li_{4/3}Ti_{5/3}O_4$/L333 cell at room temperature and 55 °C are given in Fig. 4(a). At 55 °C, the redox reaction peak takes place at a lower potential and ends

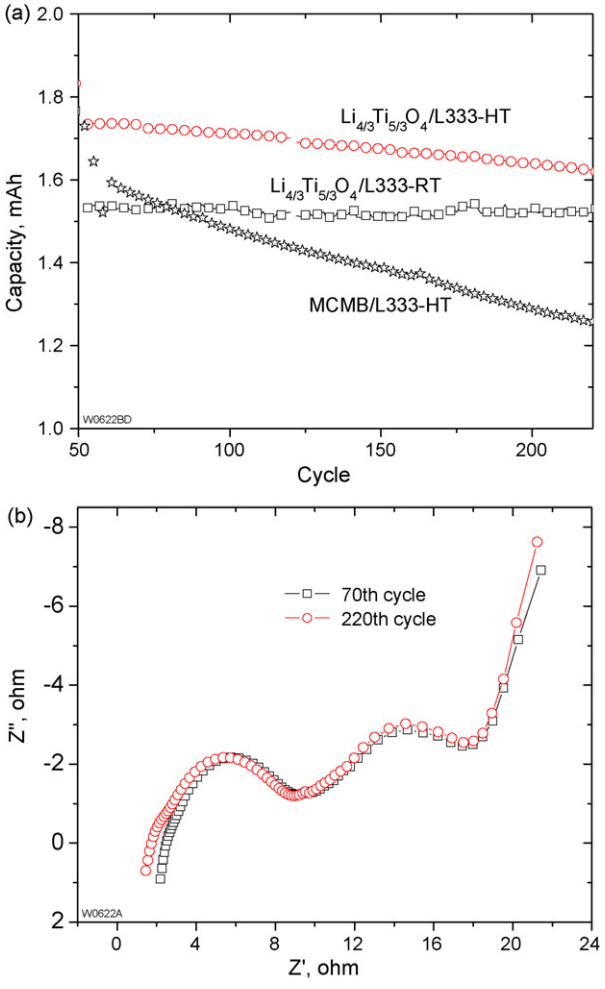

Fig. 3. (a) Capacity retention of $Li_{4/3}Ti_{5/3}O_4$/L333 cell at room temperature and elevated temperature at 1*C* rate and (b) ac impedance results of $Li_{4/3}Ti_{5/3}O_4$/L333 cell at 50% SoC after different cycles at elevated temperature.

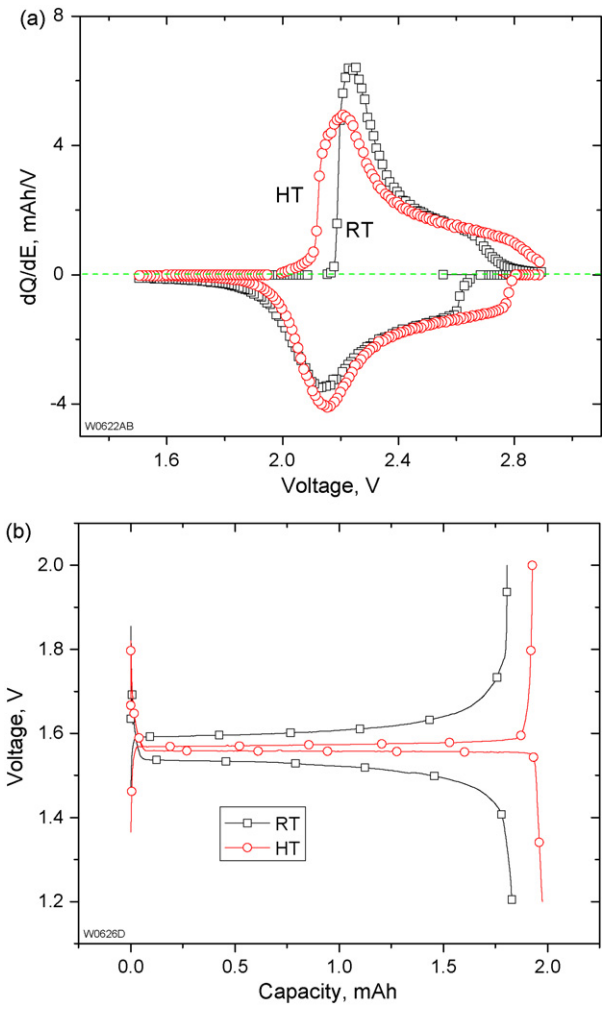

Fig. 4. (a) Differential capacity plots of $Li_{4/3}Ti_{5/3}O_4$/L333 cell and (b) voltage profiles of Li/$Li_{4/3}Ti_{5/3}O_4$ cells at room temperature and elevated temperature.

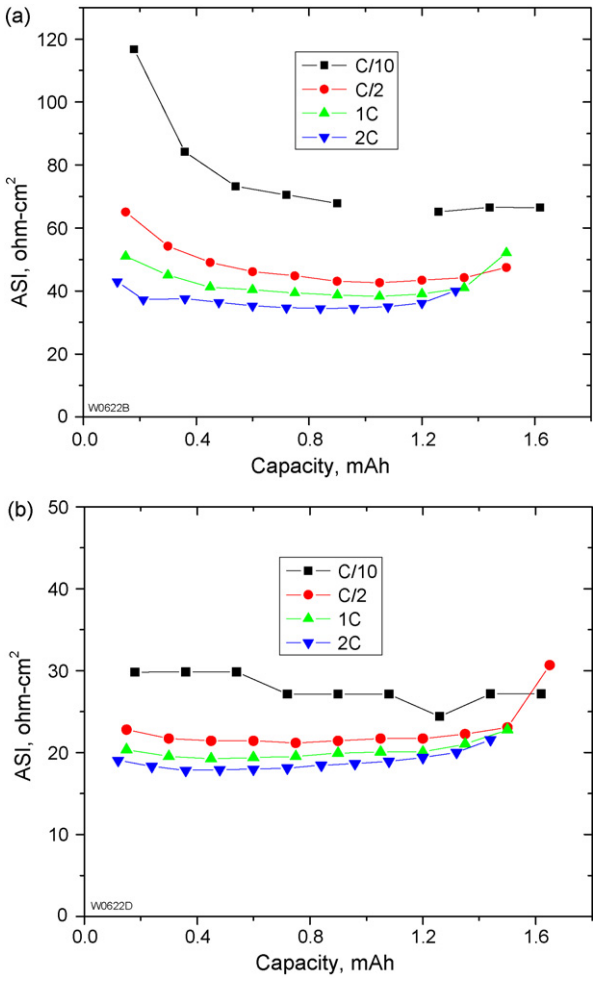

Fig. 5. ASI results of $Li_{4/3}Ti_{5/3}O_4$/L333 cell at different *C* rates under: (a) room temperature and (b) elevated temperature.

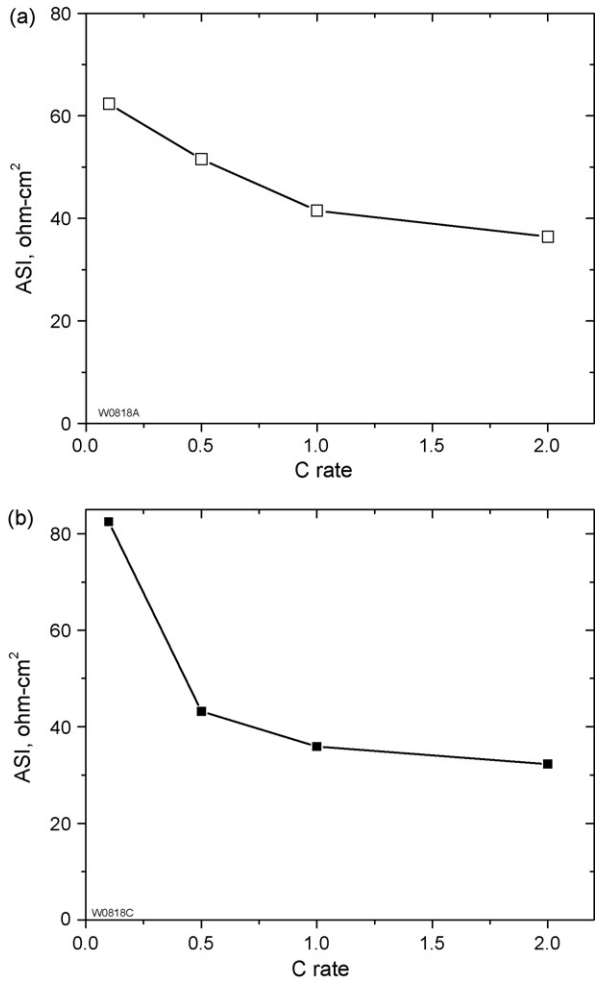

Fig. 6. ASI results of (a) Li/$Li_{4/3}Ti_{5/3}O_4$ and (b) Li/L333 cells as a function of *C* rate at 50% SoC.

at a higher potential than at room temperature. This result indicates better kinetics and explains the high capacity observed at 55 °C compared with room temperature, as shown in Fig. 3(a). As discussed in Fig. 1(a), the charge capacity is controlled by the voltage profile of $Li_{4/3}Ti_{5/3}O_4$; the lower polarization of $Li_{4/3}Ti_{5/3}O_4$ is expected to be responsible for the higher capacity obtained for the full cell at the elevated temperature. This conclusion can be confirmed by the voltage profile of the Li/$Li_{4/3}Ti_{5/3}O_4$ cell at room and elevated temperatures presented in Fig. 4(b). At the elevated temperature, the cell voltage profile is flat with less overpotential, which results in more usable capacity with the same cut-off voltage window during the charge and discharge processes for the $Li_{4/3}Ti_{5/3}O_4$/L333 cell.

The ASI results of the $Li_{4/3}Ti_{5/3}O_4$/L333 cells as a function of discharge rate at room and elevated temperatures are shown in Fig. 5(a) and (b), respectively. The impedance of the cells at different temperatures decrease with the increase in the rate, which indicates that the impedance is dominated by the electrochemical kinetics instead of by lithium-ion diffusion across the interface [18]. This electrochemical characteristic makes $Li_{4/3}Ti_{5/3}O_4$/L333 cells very suitable for high power applications, such as hybrid electric vehicles, because of the low impedance during very high current pulses.

In order to differentiate the impedance contribution from the anode and the cathode, the Li/$Li_{4/3}Ti_{5/3}O_4$ and Li/L333 half-cells were tested at room temperature. The ASI results of the Li/$Li_{4/3}Ti_{5/3}O_4$ and Li/L333 cells as a function of rate at 50% SoC are given in Fig. 6(a) and (b), respectively. For both half-cells, the impedance decreases when the testing current increases, which indicates that the Butler–Volmer kinetic effect is dominant in both half-cells. On the other hand, the ASI value of the Li/333 cell reaches equilibrium faster than that of the Li/$Li_{4/3}Ti_{5/3}O_4$ cell. This demonstrates that the power performance of the Li/$Li_{4/3}Ti_{5/3}O_4$ cell can be improved further when a higher rate is applied.

The rate capability of Li/L333 and Li/$Li_{4/3}Ti_{5/3}O_4$ cells at room temperature is shown in Fig. 7. The Li/L333 cell shows good rate capability with good capacity retention up to a 6*C* rate, as reported elsewhere [11]. By comparison, the Li/$Li_{4/3}Ti_{5/3}O_4$ cell shows much better rate capability with over 60% capacity retention when the cell is cycled continuously at a 8*C* rate. The good capacity retention of the Li/$Li_{4/3}Ti_{5/3}O_4$ cell at high rate is due to the flat cell voltage profile, which can allow it to reach

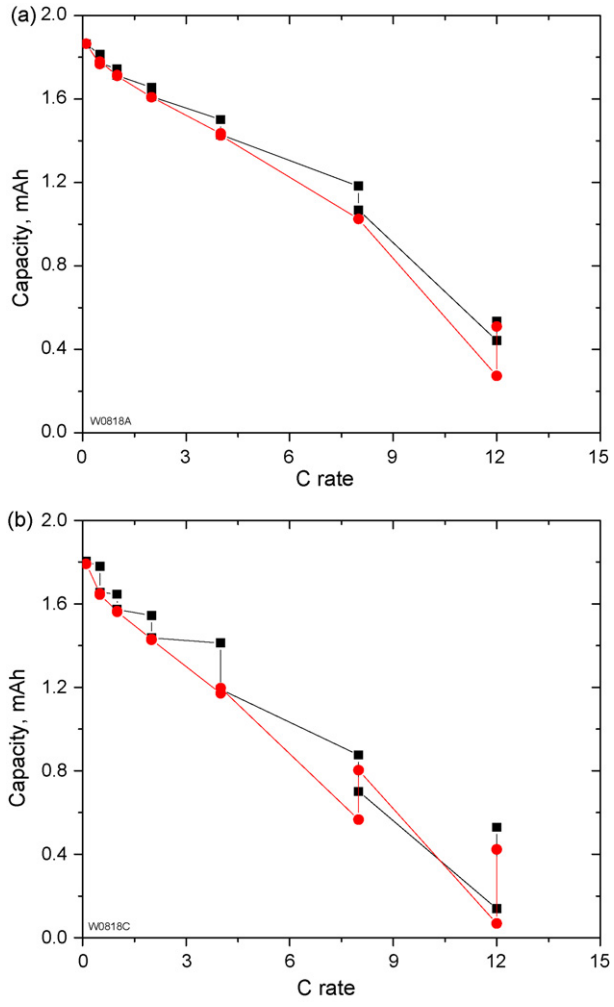

Fig. 7. Capacity retention as a function of *C* rate of (a) Li/$Li_{4/3}Ti_{5/3}O_4$ and (b) Li/L333 cells.

full cell capacity even when the cell polarization increases. Furthermore, when the cell current increases, the cell impedance decreases, which leads to the better rate capability of the system, because the impedance of the Li/$Li_{4/3}Ti_{5/3}O_4$ and Li/L333 cells is controlled by the electrochemical kinetics (Fig. 7).

4. Conclusions

The use of $Li_{4/3}Ti_{5/3}O_4$ and L333 as electrode materials in lithium-ion batteries provides an easy monitoring of cell overcharge and discharge because of the rapid voltage drop of both $Li_{4/3}Ti_{5/3}O_4$ and L333 at the end of charge and discharge. This system shows excellent capacity retention at both room temperature and at 55 °C. Unlike the carbon anode, for which significant reactivity with the electrolyte takes place at the interface the $Li_{4/3}Ti_{5/3}O_4$ electrode shows excellent stability with no rise in interfacial impedance when the cell is cycled at 55 °C. Area specific impedance studies on the full- and half-cells at different *C* rates reveal that the electrochemical kinetic is dominant. As a result, this system is very suitable for high-power applications.

Acknowledgements

This work was performed under the auspices of the U.S. Department of Energy, Energy Efficiency and Renewable Energy, Office of Freedom CAR and Vehicle Technologies, under Contract No. W-31-109-Eng-38.

References

[1] T. Ohzuku, A. Ueda, N. Yamamoto, J. Electrochem. Soc. 142 (1995) 1431.
[2] C.H. Chen, J.T. Vaughey, A.N. Jansen, D.W. Dees, A.J. Kahaian, T. Goacher, M.M. Thackeray, J. Electrochem. Soc. 148 (2001) A102.
[3] M. Venkateswarlu, C.H. Chen, J.S. Do, C.W. Lin, T.C. Chou, B.J. Hwang, J. Power Sources 146 (2005) 204.
[4] A.D. Robertson, H. Tukamoto, J.T.S. Irvine, J. Electrochem. Soc. 146 (1999) 3958.
[5] A.N. Jansen, A.J. Kahaian, K.D. Kepler, P.A. Nelson, K. Amine, D.W. Dees, D.R. Vissers, M.M. Thackeray, J. Power Sources 81/82 (1999) 902.
[6] X.L. Yao, S. Xie, C.H. Chen, Q.S. Wang, J.H. Sun, Y.L. Li, S.X. Lu, Electrochim. Acta 50 (2005) 4076.
[7] J. Jiang, J. Chen, J.R. Dahn, J. Electrochem. Soc. 151 (2004) A2082.
[8] D.D. MacNeil, J.R. Dahn, J. Electrochem. Soc. 149 (2002) A912.
[9] I. Belharouak, K. Amine, Electrochem. Commun. 5 (2003) 435.
[10] W. Lu, I. Belharouak, D. Vissers, K. Amine, J. Electrochem. Soc. 153 (2006) 2147.
[11] I. Belharouak, Y.-K. Sun, J. Liu, K. Amine, J. Power Sources 123 (2003) 247.
[12] I. Belharouak, W. Lu, D. Vissers, K. Amine, Electrochem. Commun. 8 (2006) 329.
[13] B.J. Hwang, Y.W. Tsai, D. Carlier, G. Ceder, Chem. Mater. 15 (2003) 3676.
[14] Z. Chen, Y.-K. Sun, K. Amine, J. Electrochem. Soc. 153 (2006) 1818.
[15] Z.H. Chen, W. Lu, J. Liu, K. Amine, Electrochim. Acta 51 (2006) 3322.
[16] W. Lu, Z.H. Chen, H. Joachin, J. Prakash, K. Amine, J. Power Sources 161 (2006) 1074–1079.
[17] W. Lu, unpublished results.
[18] D. Dees, E. Gunen, D. Abraham, A. Jansen, J. Prakash, J. Electrochem. Soc. 152 (2005) 1409.